Thermodynamic stability of PuO_2 surfaces: Influence of electronic correlations

Gérald Jomard* and François Bottin
CEA, DAM, DIF, F-91297 Arpajon, France

(Received 8 June 2011; revised manuscript received 5 September 2011; published 29 November 2011)

In this article, we performed accurate *ab initio* calculations in order to address the influence of electronic correlations on the surface stability of PuO_2. Various terminations of the (100), (110), and (111) orientations were considered, among which some are polar. Standard density-functional theory (DFT), which is known to provide a poor description of the electronic structure of plutonium oxides, predicts an unexpected stabilization of the polar uncompensated terminations O_2-(111) and Pu-(111). We show that this shortcoming is no longer observed when the more relevant PBE + U framework is used. The so-obtained better description of the strong electronic correlations leads to a destabilization of these two terminations, leaving only one stable surface, the O-(111) stoichiometric one. Beyond the surface stability, we show that the electronic structure is strongly affected since the PBE + U approach is able to render only a proper insulating behavior. This should have a strong effect on the surface reactivity of these systems and prevent the use of standard DFT.

DOI: 10.1103/PhysRevB.84.195469 PACS number(s): 68.35.Md, 68.47.Gh, 71.15.Mb, 71.27.+a

I. INTRODUCTION

Plutonium-based materials attract much interest, due to their technological and environmental implications,[1,2] as well as for theoretical prospects. PuO_2 is used, in particular, as a constituent of nuclear reactor fuels and stands as an important compound, with regard to the very long-term storage of plutonium. From an experimental standpoint, the chemical reactivity of elemental plutonium is highly complex, involving strong, rapid corrosion of samples in a variety of outside environments. Consequently, the reactivity of plutonium metal, oxides, and hydrides has become a significant field of research over the past decade.[3–11]

With regard to theoretical calculations, the electronic structure of these correlated materials still poses a challenge for electronic simulations. Indeed, the elemental plutonium metal stands at the boundary between two types of electronic behavior, as the actinides series progresses, passing from itinerant to localized 5f states.[1,12–14] The early, light, actinides exhibit a transition-metal-like behavior, with f electrons hybridizing with each other. By contrast, the later, heavy, actinides show a lanthanide-like aspect, with f electrons localized in the atoms. While the former is adequately described by means of conventional band-structure calculations, e.g., within density-functional theory (DFT), in the standard local-density approximation (LDA), or the generalized gradient approximation (GGA), the latter form proves more challenging. In particular, conventional local density-functional theory does not capture the localization effect of the f electrons arising from the strong electron-electron interaction.

In order to circumvent this shortcoming, various approaches have been proposed and applied to plutonium and its oxides, e.g., calculations involving a self-interaction correction (SIC),[15,16] hybrid exchange-correlation functionals,[17,18] or intra-atomic Coulomb interaction.[19–25] The latter is known as the LDA + U approach,[26–29] which has been used extensively for a wide panel of correlated materials. A more general formalism, using a combination of dynamical mean-field theory (DMFT),[27,30,31] together with LDA, appears to be highly promising, as regards such correlated materials.[32–35]

In the present article, the atomic and electronic structures of a large number of terminations of PuO_2 is analyzed. This work is performed by means of *ab initio* calculations, with or without use of a Hubbard U parameter. To assess the relative thermodynamic stability of these terminations as a function of the temperature and oxygen partial pressure, the technique of *ab initio* atomistic thermodynamics is employed. In particular, we show how this stability evolves from GGA to GGA + U calculations and how these modifications are related to a better description of the surface electronic structure. At last, a tentative explanation of peculiar electronic features appearing on the surface of such correlated materials is proposed.

II. METHODOLOGY

A. Terminology about surface and terminations

As an initial attempt to study the surface properties of PuO_2, we choose to consider only (1 × 1) surface unit cells and low-index surfaces, e.g., (100), (110), and (111). Along the [110] direction, the fluorite crystal consists in a stacking sequence of planes, -PuO_2-PuO_2-PuO_2-. In the ionic limit, with each PuO_2 plane being "charge neutral," the (110) orientation is called nonpolar. If the crystal is cleaved in a (110) plane, two equivalent surfaces are obtained, named PuO_2-(110) in the following (see Fig. 1).

Along the [100] and [111] directions, the sequence is -Pu-O_2-Pu-O_2-Pu-O_2-. In the ionic limit, the O_2 and Pu planes bear a $\pm 4e$ charge and these orientations are called polar. By cleaving the crystal through these planes, two terminations may be created: the O_2-(111) and Pu-(111) or the O_2-(100) and Pu-(100) terminations, respectively (see the first two rows of Figs. 2 and 3).

When dealing with polar oxide surfaces (see Refs. 36 and 37 and references therein), it should be borne in mind that a repeated sequence of dipoles (an alternating sequence of charge), from bulk to surface, leads to a divergence of the electrostatic potential when the number of sequences tends to infinity. The only way to overcome this instablility is to have a reduction of the surface charge (in this case, a $\pm 2e$ surface charge is needed). This can be achieved either (i) through a modification of the surface electronic structure,

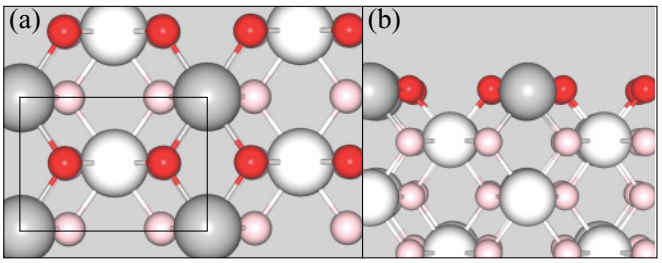

FIG. 1. (Color online) Top (a) and side (b) views of the nonpolar PuO_2-(110) surfaces.

leading to an open-shell structure, or (ii) through a modification of the surface atomic structure, which is energetically more favorable.

Here, the first mechanism applies to the O_2- and Pu-(111) and (100) terminations. The second one can be considered by removing a few atoms from (or adding a few atoms to) the surface planes and achieving the charge compensation ($\pm 2e$). If, in general, a large number of surface reconstructions obey

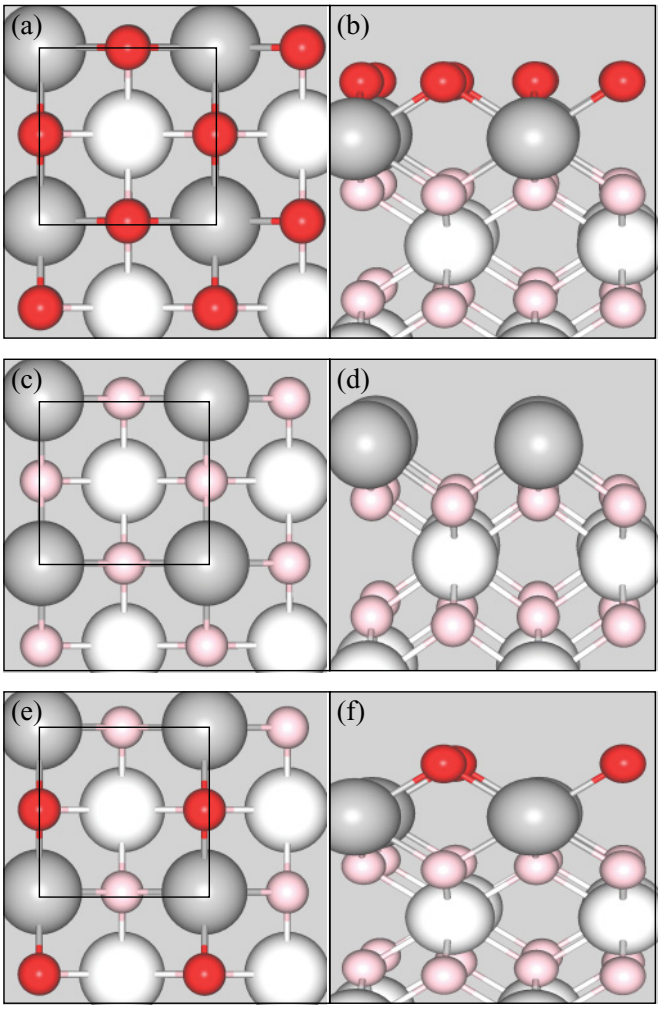

FIG. 2. (Color online) Top (left) and side (right) views of various terminations of PuO_2-(100) surfaces: [(a) and (b)] the polar and noncompensated O_2 termination, [(c) and (d)] the polar and noncompensated Pu termination, and [(e) and (f)] the polar and compensated O termination.

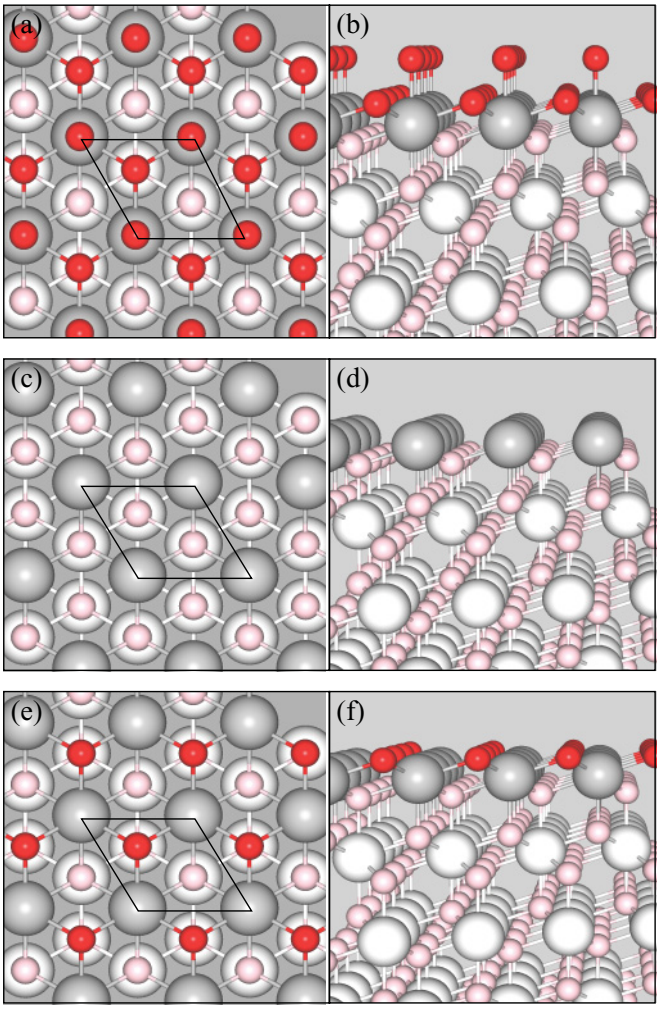

FIG. 3. (Color online) Top (left) and side (right) views of various terminations of PuO_2-(111) surfaces: [(a) and (b)] the polar and noncompensated O_2 termination, [(c) and (d)] the polar and noncompensated Pu termination, and [(e) and (f)] the polar and compensated O termination.

to this constraint (see the example of ZnO),[38] in the framework of (1×1) surface unit cell only the O-(111) and O-(100) terminations can be created. These ones will be named "polar and compensated" in the following since the polar instability is healed through a modification of the surface stoichiometry, whereas the O_2- and Pu-(111) and (100) terminations will be named "polar and noncompensated" since a modification of the surface electronic structure is expected to occur.

B. *Ab initio* simulations parameters

This study was carried out using the ABINIT package.[39,40] We used the projector augmented wave (PAW) formalism, which affords the accuracy of all electron methods (the nodal structure of wave functions is correct), and is efficient with regard to the structural relaxation of large systems.[41] The PAW data sets used for plutonium and oxygen were generated with the ATOMPAW code[42] (see our previous work[25] for more details). These atomic data do not provide for any overlap between neighboring PAW spheres for plutonium oxides. All computational parameters were carefully selected

to yield a total energy convergence better than 1 meV/atom. In particular, we use an energy cutoff equal to 24 Ha and a $6 \times 6 \times 6$ Monkhorst-Pack (M-P) **k**-point sampling mesh[43] of the Brillouin zone for the bulk calculations.

Each surface is modeled by way of the slab model and allowed to relax. In order to ensure a convergence of surface energies better than 10 mJ/m^2, slabs with a stacking of six PuO_2 formula units separated by 15 Å of vacuum are found to be sufficient. The Brillouin zone of the (100), (110), and (111) slabs are sampled by $(6 \times 6 \times 2)$, $(6 \times 4 \times 2)$, and $(7 \times 7 \times 2)$ M-P meshes, leading to calculations with 9, 6, and 28 **k** points, respectively. Therefore, a massive use of the three levels of parallelization available in the ABINIT code is performed.[44]

In the near future, we will address the interaction arising between PuO_2 surfaces and some of the gases present in the atmosphere. For that reason, we adopted the Perdew-Becke-Ernzerhof (PBE) exchange and correlation functional,[45] since this one is more relevant than LDA, for the purpose of describing cohesion in gaseous molecules. However, this functional is known to provide a poor description of the electronic structure of plutonium oxides. Recently,[25] we showed that the introduction of an intra-atomic Coulomb interaction[46] allows this shortcoming to be corrected for. In this work, a couple of $U = 4.0$ eV and $J = 0.7$ eV parameters is selected, yielding to an acceptable overall agreement between experiments and theory as regards the physical properties of bulk Pu, Pu_2O_3, and PuO_2.[25] As our main objective is to address the effect of strong electronic correlations on the PuO_2 surface stability, we performed both PBE and PBE+U calculations. For each case we have considered the magnetic ordering that is predicted for the ground state of the bulk phase: ferromagnetic (FM) within the standard DFT approach and antiferromagnetic (**1k** AFM) when the Hubbard correction is applied. The respective theoretical equilibrium lattice parameters used to performed the slab calculations were $a_0^{\mathrm{PBE}} = 3.82$ Å and $a_0^{\mathrm{PBE}+U} = 3.85$ Å (see Ref. 25).

Applying the **1k** AFM ordering to the slabs used to model the (110) and (100) surfaces is straightforward. We simply consider alternating magnetic moments along the normal of the surface plane. However, in the specific case of the (111) orientation, in order to accomodate the **1k** AFM ordering, one should use a nonprimitive surface supercell that would strongly increase the computational cost. We have, thus, decided to use an another AFM ordering consisting of alternating moments along the $\langle 111 \rangle$ direction. Obviously, we first checked that the energy difference between these two different AFM orderings was acceptable (on the order of 1 meV/atom, i.e., in the range of the error due to other approximations).

In order to deal with the notorious metastable-states problems that are frequently encountered in DFT + U applications, we apply the solution we proposed in earlier works.[25,47] More specifically, in this study, (i) we start the atomic structure relaxation of the slabs by fixing during 20 electronic steps the occupation matrix found to give the global minimum of the bulk ground state, then (ii) release this constraint until the end of the electronic minimization, and, finally, (iii) at the end of the atomic structure relaxation, control *a posteriori* that the 5f orbital occupancies of the Pu atoms of the central planes were very close to the one identified for the bulk ground state. By performing a convergence with respect to the thickness of the slab we are also able to ensure *a posteriori* that surface states far from the bulk one are not trapped within metastable states.

At last, we must stress that our calculations are restricted to a scalar relativistic level. We do not include spin-orbit coupling (SOC). The plutonium element being an heavy metal, spin-orbit interaction is expected to be important for the physics of its compounds. However, very recently, Nakamura *et al.*[48] have shown that, for what concerns the description of a gap in the electronic density of states (DOS), the SOC is of second-order effect compared to the Hubbard correction. We will show in the following that the surface stabilities in PuO_2 are closely linked to the presence of a gap in the DOS. Therefore, we do not expect SOC to change the conclusions of this work and choose to neglect this effect in a first approach.

C. *Ab initio* atomistic thermodynamics

For the purpose of comparing the stability of various terminations in a monoatomic solid, we want to compute surface energy. For a polyatomic crystal this quantity is defined only for stoichiometric slabs; i.e., for PuO_2-(110), O-(100), and O-(111) terminations. If E^i_{slab} is the total energy of the slab modeling the i termination, $E^{\mathrm{PuO_2}}_{\mathrm{bulk}}$ the total energy per atom of the PuO_2 bulk crystal, A the surface unit area, and $N_{\mathrm{PuO_2}}$ the number of PuO_2 unit formula contained in the slab, the surface energy of the i termination reads as follows:

$$E^i_{\mathrm{surf}} = \frac{1}{2A}\left(E^i_{\mathrm{slab}} - N_{\mathrm{PuO_2}} E^{\mathrm{PuO_2}}_{\mathrm{bulk}}\right). \tag{1}$$

Obviously, for nonstoichiometric slabs [i.e., for O_2- and Pu-(100) and (111) terminations], this quantity cannot be used, since $N_{\mathrm{PuO_2}}$ is undefined. Instead, the surface grand potential, an excess quantity that generalizes the concept of surface energy, must be applied. This quantity has been widely used, of late, to study binary[49] as well as ternary[50] compounds. For the specific case of PuO_2, the surface grand potential of the i termination is expressed as follows:

$$\gamma^i_{\mathrm{surf}} = \frac{1}{2A}\left[\Omega^i_{\mathrm{slab}} - N_{\mathrm{PuO_2}} \Omega^{\mathrm{PuO_2}}_{\mathrm{bulk}}\right]. \tag{2}$$

The grand potential of the slab modeling the i termination and the bulk PuO_2 are, respectively,

$$\Omega^i_{\mathrm{slab}} = F^i_{\mathrm{slab}} - \sum_j \mu_j N_j, \tag{3}$$

$$\Omega^{\mathrm{PuO_2}}_{\mathrm{bulk}} = F^{\mathrm{PuO_2}}_{\mathrm{bulk}} - \mu_{\mathrm{PuO_2}}, \tag{4}$$

where N_j and μ_j are, respectively, the number and the chemical potential of the j species that composed the slab. Considering that configurational and vibrational contributions to entropy are almost equal in the bulk and the slab,[51] and cancel each other in Eq. (2), we can replace the free energies F by their total energies E counterparts. These contributions would be needed to resolve, as a function of the temperature, an inversion of stability between two terminations separated by a few tens of meV.[52–54] The surface energies found in this work are well separated by a few hundreds of meV and these contributions can be safely neglected in a first approximation.

Doing that, the surface grand potential has no more explicit temperature dependence but keeps an implicit one via the oxygen chemical potential. The $\mu_O(p,T)$ can be easily

expressed as a function of the temperature T and the oxygen partial pressure p using the ideal gas approximation. In its relative form, this one reads as follows:

$$\Delta\mu_O(p,T) = \tfrac{1}{2}\left[E_{\rm mol}^{O_2} + \bar{\mu}_{O_2}(p^0,T) + k_B T \ln(p/p^0)\right], \quad (5)$$

where $E_{\rm mol}^{O_2}$ is the total energy of a molecule in the gas phase (We choose the O_2 dimer as a reference for oxygen. The calculations of an isolated molecule have been performed in the DFT-PBE framework. As is well known, this leads to an overestimation of the binding in the molecule (see, for example, Ref. 25) but, due to error cancellation in the computation, we expect the surface grand potentials to be only slightly affected), p^0 is a reference pressure (here 1 atm), and $\bar{\mu}_{O_2}(p^0,T)$ includes all the contributions coming from the molecule rotations and vibrations. In the present work, this quantity is not evaluated using first-principles calculations but is taken from experimental values, as listed in thermochemical tables.[55]

At last, if we assume that the surface stands in chemical and thermodynamical equilibrium with PuO_2 (the bulk acting as a reservoir), this entails the following relation:

$$\mu_{PuO_2} = \mu_{Pu} + 2\mu_O = E_{\rm bulk}^{PuO_2}. \quad (6)$$

We introduce this last relation within Eq. (2), remove the dependence coming from the plutonium chemical potential, and obtain:

$$\begin{aligned} \gamma_{\rm surf}^i &= \phi_{\rm surf}^i - \alpha^i \Delta\mu_O, \quad \text{with} \\ \phi_{\rm surf}^i &= \frac{1}{2A}\left[E_{\rm slab}^i - N_{Pu}E_{\rm bulk}^{PuO_2} - \frac{E_{\rm mol}^{O_2}}{2}(N_O - 2N_{Pu})\right] \quad (7) \\ \alpha^i &= \frac{1}{2A}(N_O - 2N_{Pu}). \end{aligned}$$

For each termination we compute its surface grand potential, defined as a straight line, with all the *ab initio* results included within the y intercept $\phi_{\rm surf}^i$ and the slope α^i defining the excess or the deficit in oxygen on the surface.

The surface grand potential is not defined over the whole range of variation of the relative chemical potential $\Delta\mu_O$. One has to ensure that both the PuO_2 compound and oxygen in the condensed phase are thermodynamically stable. This gives the following lower and upper boundaries, respectively:

$$E_f^{PuO_2} = E_{\rm bulk}^{PuO_2} - E_{\rm bulk}^{Pu} - E_{\rm mol}^{O_2} < \Delta\mu_O < 0\text{eV}, \quad (8)$$

where $E_{\rm bulk}^{Pu}$ is the total energy of plutonium in its δ phase. In our previous work[25] we showed that $E_f^{PuO_2}$ equals -9.70 and -10.14 eV in PBE and PBE$+U$ calculations, respectively, the last value being in better agreement with experiment (-10.36 eV). In addition, we have to prevent the formation of a Pu_2O_3 compound, which can be performed by imposing

$$E_r^{Pu_2O_3\to PuO_2} = 2E_f^{PuO_2} - E_f^{Pu_2O_3} < \Delta\mu_O. \quad (9)$$

The reaction energy $E_r^{Pu_2O_3\to PuO_2}$ is equal to -4.06 and -4.10 eV in GGA and GGA$+U$ calculations,[25] values which are slightly smaller than the experimental value -4.32 eV set in the following. Below this value, in an oxygen-poor environment, the PuO_2 is not stable with respect to the formation of the plutonium sesquioxide, which restricts the range of variation of the relative oxygen chemical potential to $-4.32 < \Delta\mu_O < 0$ eV.

III. RESULTS

The surface energies $\phi_{\rm surf}^i$ of seven i terminations [see Eq. (7)] are listed in Table I for ideal and relaxed systems. Two sets of results are presented. The first one covers PBE calculations while the second one corresponds to PBE$+U$ calculations. In each case we considered the proper ground state which is, respectively, FM and AFM.

A. Comparison with other works

We will first discuss the PBE results in Table I for the O-(111), O-(100), and PuO_2-(110) terminations. In these cases, the surface grand potential is equal to the surface energy [as computed using Eq. (1)]. Among the stoichiometric surfaces, we find O-(111) to be the most stable. Negligible relaxations are found for this highly compact surface. On the other hand, the very open O-(100) surface is strongly affected by relaxation, with the gain in energy being around 0.52 J/m^2. The relative ordering of stoichiometric surface stabilities, after relaxation, is (111) > (110) > (100). Using conventional ion-pair potentials, Tan and coworkers[56] find the same ordering, although the absolute values may be 2 times larger than our PBE results (see Table I). This ordering seems to be clearly established for dioxides that crystallize in the fluorite structure, since it is also reported for CeO_2[57] and UO_2.[56] It is, thus, satisfactory that this ordering is recovered by our approach. To the best of our knowledge, DFT-based studies of PuO_2 surfaces are very scarce in the literature. It seems that only Wu and Ray have explored this system. They restricted their study to the PuO_2-(110) surface, considering an FM state for the PuO_2 crystal.[58–60] Unfortunately, they did not report the surface energy. They mention only the surface energy relaxation, which, in GGA, stands at 0.268 eV per unit cell, when only atoms in the outermost planes are relaxed,[58–60] and at 0.53 eV per unit cell, when the five planes of their slab were allowed to relax.[9] By converting the values in Table I to the same units, surface energy relaxation is found to stand around 0.58 eV per unit cell in our study. This involves a difference of only 0.05 eV compared to their result. This discrepancy is not readily accounted for but it may probably attributed to the difference of exchange and correlation energy functionals, PW91 vs. PBE. We repeated these calculations within the

TABLE I. PuO_2 surface energies, $\phi_{\rm surf}^i$, in J/m^2, computed within the PBE and PBE$+U$ frameworks for seven i terminations. Results obtained by Tan and coworkers[56] are shown for comparison.

	110	100			111		
	PuO_2	O_2	O	Pu	O_2	O	Pu
	Unrelaxed						
PBE FM	1.33	2.01	2.17	5.78	3.60	0.75	6.47
PBE$+U$ AFM	1.41	3.21	2.35	6.12	4.59	0.74	7.06
	Relaxed						
PBE FM	1.10	0.68	1.64	5.32	0.60	0.74	5.49
PBE$+U$ AFM	1.13	2.76	1.69	5.88	3.05	0.72	6.29
Ionic potentials (Ref. 56)	2.20		2.92			1.39	

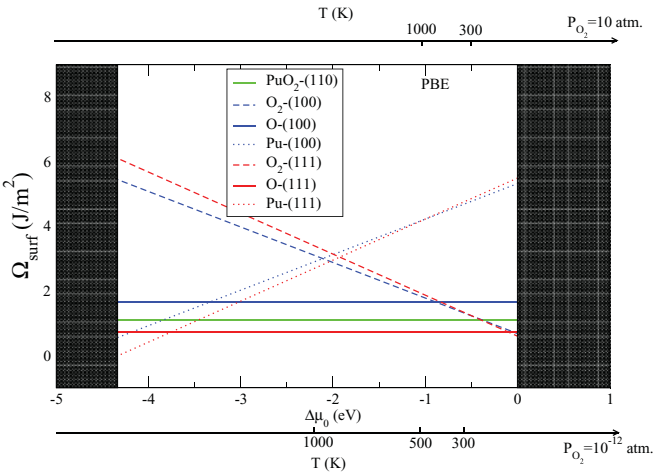

FIG. 4. (Color online) PBE-calculated surface grand potentials for the various PuO_2 surfaces considered as a function of oxygen chemical potential $\Delta\mu_O$ (the corresponding temperature scales are shown for oxygen partial pressures of 10 and 10^{-12} atm).

PBE + U framework. It may be seen, in Table I, that the relative ordering of stoichiometric surface stabilities is unchanged. The main differences are found for the nonstoichiometric surfaces and will be discussed in the following.

B. Thermodynamic stability

The respective dependence of the surface grand potentials on the oxygen chemical potential, as obtained from Eq. (7) using our PBE and PBE + U calculations, is set out in Figs. 4 and 5. Together with the oxygen chemical potential, we show two temperature scales, corresponding to oxygen partial pressures equal to 10 and 10^{-12} atm. The surface grand potentials $\Omega(T, p)$ derived from the PBE calculations are consistent with the stabilization of the nonstoichiometric O_2-(111) termination in oxygen-rich environments (very low temperature and high oxygen partial pressure). Above, the stoichiometric O-(111) termination is favored until extremely high temperatures for which we predict a stabilization of the Pu-terminated (111) surface. The presence of these two

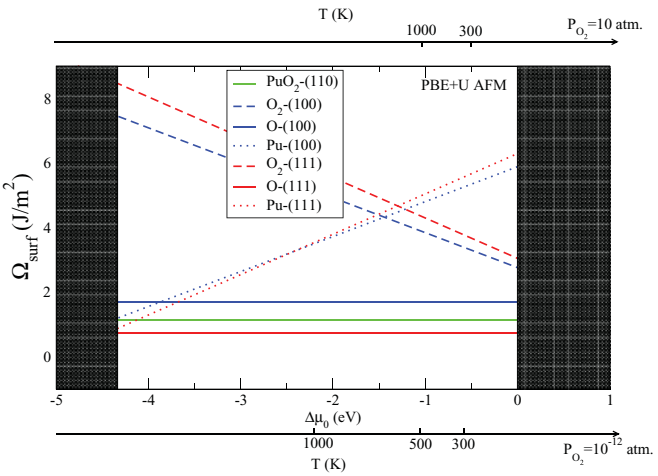

FIG. 5. (Color online) Same as described in the caption to Fig. 4 but for PBE + U calculations.

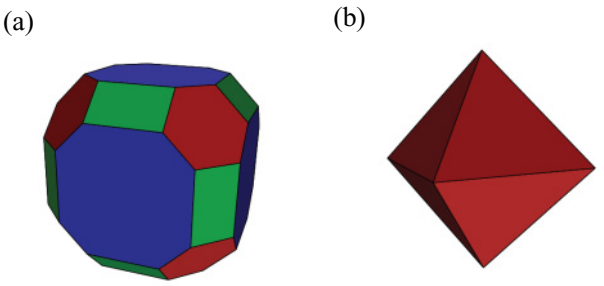

FIG. 6. (Color online) Equilibrium crystal shape of (a) an arbitrary cubic crystal and (b) a PuO_2 nanocrystal for an oxygen partial pressure and a temperature equal to $P = 1$ atm and $T = 300$ K, respectively. The (100), (110), and (111) facets are shown in blue, green, and red, respectively.

polar and noncompensated O_2- and Pu-(111) terminations in the phase diagram of PuO_2 surfaces is quite unexpected as mentioned in Sec. II A. We surmise that this behavior is due to the inability of DFT to provide a correct description of the electronic structure of these systems (in this framework, all the slabs are metallic as can be seen for example in Fig. 7). This assumption is supported by our PBE + U-based results, shown in Fig. 5. Indeed, within this framework, the nonstoichiometric O_2-terminated surfaces, O_2-(100) and O_2-(111), are greatly destabilized. As a consequence, the PBE + U-derived surface free energies are consistent with a stabilization of the O-(111) termination over the entire range of temperatures, regardless of oxygen partial pressure.

Using the Gibbs-Wulff theorem of equilibrium crystal shape (ECS)[61] and the computed surface energies, the morphology of PuO_2 nanocrystals as a function of oxygen chemical potential may be predicted. This is achieved by minimizing the total free energy $\mathcal{F}_A$ of the crystal at a constant volume:

$$\mathcal{F}_A = \iint_{A(V)} \gamma(\vec{n}) dA, \tag{10}$$

where $\gamma(\vec{n})$ stands for the surface free energy, $\vec{n}$ is the surface normal, A is the surface area of the crystal, and V its volume. Figure 6 shows the general shape that can be obtained for a cubic crystal when only (100), (110), and (111) facets are considered. For the purpose of studying the crystal morphology of PuO_2 nanocrystals, we opted to focus on normal oxygen partial pressure and temperature conditions ($P = 1$ atm, $T = 300$ K). Further, we described only the equilibrium crystal shape based on our PBE + U free energies. In these conditions, the predicted ECS shown in Fig. 6(b) exhibits (111) facets only. This can be connected to the energy values obtained for the three stoichiometric terminations O-(111), PuO_2-(110), and O-(100), the first one departing strongly from the two latter over the entire temperature regime, whatever the value of the oxygen partial pressure.

C. Electronic structure

In order to study the electronic structures of the PuO_2 surfaces, we have computed the orbital-projected density of states (pDOS) for each of the above-mentioned orientations using either the standard DFT-PBE framework or the PBE + U one. The results are represented in Figs. 7 and 8.

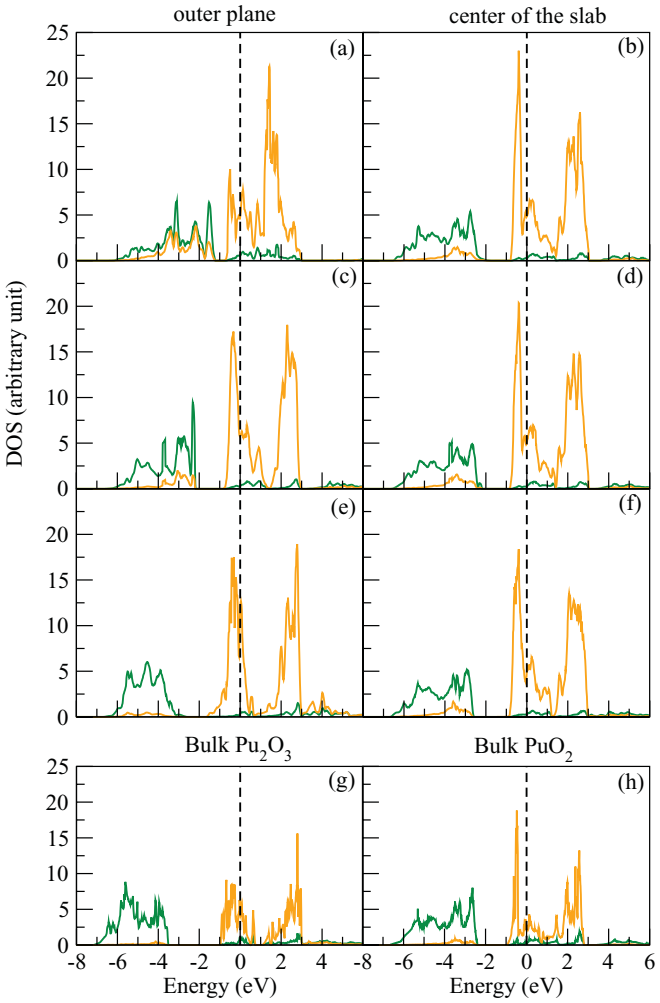

FIG. 7. (Color online) The PBE-FM calculated pDOS for the Pu $5f$ and O $2p$ orbitals are shown, respectively, in orange and in green. Note that the Fermi level has been shifted to zero. Panels (a), (c), and (e) correspond, respectively, to the pDOS of the surface plane of the O_2-, O-, and Pu-(111) terminations, while panels (b), (d), and (f) represent the pDOS of the central plane of the slab modeling the mentioned terminations. For comparison we have also plotted the pDOS of bulk Pu_2O_3 and PuO_2 on panels (g) and (h).

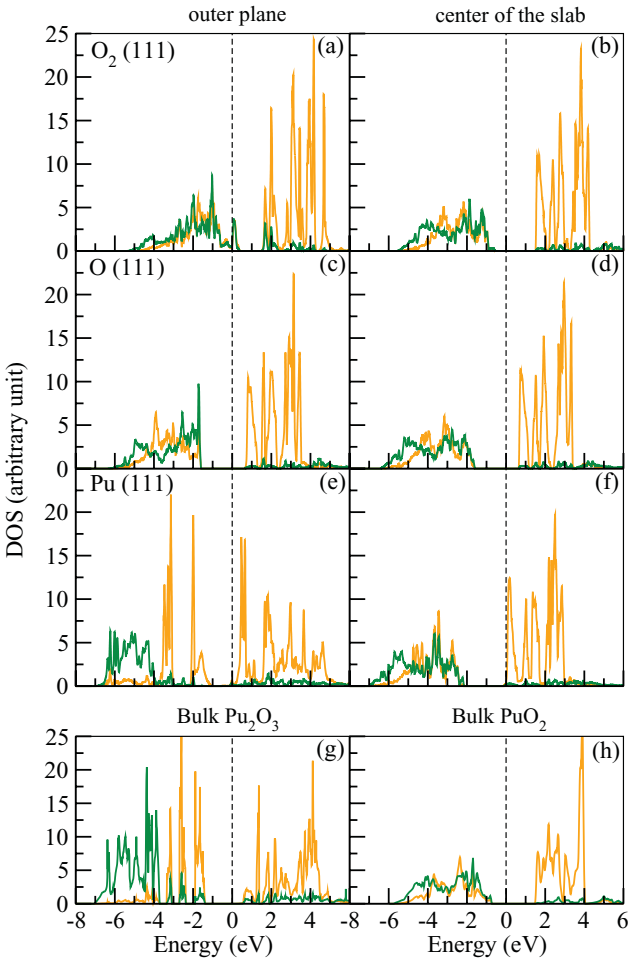

FIG. 8. (Color online) The PBE + U calculated pDOS for the Pu $5f$ and O $2p$ orbitals are shown, respectively, in orange and in green. Note that the Fermi level has been shifted to zero. Panels (a), (c), and (e) correspond, respectively, to the pDOS of the surface plane of the O_2-, O-, and Pu-(111) terminations, while panels (b), (d), and (f) represent the pDOS of the central plane of the slab modeling the mentioned terminations. For comparison we have also plotted the pDOS of bulk Pu_2O_3 and PuO_2 on panels (g) and (h).

First, we emphasize that the pDOS at the center of each slab [see Figs 7(b), 7(d), 7(f), 8(b), 8(d), and 8(f)], are very close to the pDOS of the bulk PuO_2 [see Figs. 7(h) and 8(h)]. In particular in the case of the PBE + U calculations, the center of the slabs still exhibit an insulating character. For all three terminations, the band gap is on the same order as the one obtained for the bulk, 2.1 eV (see Ref. 25). This value is slightly greater than the experimental one, 1.8 eV,[62] which is satisfactory since DFT is not designed to describe excited states. This very good agreement guarantees that the number of planes in the slabs is sufficient to recover the bulk electronic properties at their center which is a necessary condition when using the slab model.

The pDOS calculated within the DFT-PBE approach show a metallic behavior for the all three terminations. The polar and compensated O-(111) termination exhibits a surface pDOS very similar to the bulk one. This is coherent with the fact that this termination does not require a redistribution of the charge. The surface pDOS of the Pu-(111) termination is closer to the pDOS of bulk Pu_2O_3 than to the bulk PuO_2 one [compare Figs. 7(e) and 7(h)]. On the other hand, the pDOS of the O_2-(111) termination differs more strongly from the bulk case. Indeed, in Fig. 7(a), we can observe an enhancement of the O-$2p$/Pu-$5f$ hybridization as well as a decrease of the Pu-$5f$ contribution just below the Fermi level. This is the result of the surface charge redistribution imposed by the needed polarity compensation for that termination.

In the case of the pDOS calculated including the Hubbard correction, the discrepancies between each termination and between the surface and the bulk are much more visible, as we will see in the following. For what concerns the O_2-(111) termination [see Fig. 8(a)], one can readily observe an open-shell electronic strucure on the surface. It is directly due to the charge reduction (from $-4e$ to $-2e$) which is expected in order to compensate the polarity, with two surface electronic states emptied at the top of the valence

band. This is proven by a Bader charge analysis showing a strong reduction of the oxygen charge from $-1.24e$ in the bulk to $-0.62e$ and $-0.92e$ in the O_2 surface layer. At odds with PBE calculations, where the slab is metallic, in the present PBE + U calculations the bulk below the surface is (and remains) an insulator. The screening of this strong modification of the surface electronic structure is more energetically expensive than in the case of PBE calculations (see Fig. 4) and yields to a destabilization (around 2.45 J m^{-2}) of this "polar uncompensated" O_2-(111) termination with respect to the "polar and compensated" O-(111) termination (see Fig. 5).

If we now focus on the Pu-terminated (111) surface, which is also "polar and uncompensated," the analysis of its pDOS does not clearly show a reduction of the plutonium atoms of the surface plane [see Fig. 8(e)]. The surface remains insulating while we expect a reduction of the surface charge (from $+4e$ to $+2e$), with two surface electronic states filled at the bottom of the conduction band. In fact, the two additional electrons filling these surfaces states occupy $5f$ correlated plutonium orbitals that are pushed downward to the Fermi level due to the U Hubbard correction. This is clearly seen if we have a look at the local magnetic moment on each Pu atom of the slab: when this moment is around 3.9 μ_B near the center of the slab, it reaches 4.6 μ_B on the two outermost Pu planes. The compensation is, thus, achieved on two planes instead of only the extreme one. The two involved plutonium atoms stand in a Pu^{3+} oxidation state with a final pDOS, thus, very close to the one obtained for the bulk Pu_2O_3. This conclusion is also supported by the strong atomic relaxations that are observed for this particular termination. Indeed, after relaxation the outermost plane is no longer a plane of plutonium atoms but, instead, an oxygen plane. The sequence of planes near the surface is now O-Pu-O-Pu-O which is consistent with what is found in the Pu_2O_3 crystal. The surface remains insulating, and this has energetical implications. In particular, the thermodynamic stability of this "uncompensated polar" termination is not strongly modified when going from GGA (see Fig. 4) to GGA + U (see Fig. 5) calculations.

In the specific case of the polar O-terminated (111) surface, we do not expect any strong modification of the surface pDOS since this one is "compensated" regarding the polarity. This is clearly shown in Fig. 8(c) with a surface pDOS very close to the one obtained in the bulk [see Fig. 8(h)]. Finally, it is interesting to note that an improved treatment of the strong electronic correlations does not alter the thermodynamic stability of the PuO_2-(110), O-(100), and O-(111) stoichiometric terminations (see Table I). In this case, the surface electronic structure is not strongly modified with respect to the bulk, which can be metallic (in GGA) or insulating (in GGA + U), and the surface energies remain almost equal: from 1.14 to 1.13 J/m^2, from 1.70 to 1.69 J/m^2, and from 0.82 to 0.72 J/m^2, respectively. A better treatment of the electronic correlation seems to be needed only when the surface electronic structure—the oxidation state of surface elements—is modified. Conversely, *ab initio* simulations cannot be predictive for surface calculations of correlated materials without taking into account for an improved treatment of the strong electronic correlations, whatever it is.

IV. CONCLUSIONS

By means of total energy calculations within the PBE and PBE + U frameworks, we studied the thermodynamic stability of various terminations of the low-index (100), (110), and (111) surfaces of plutonium dioxide. Surface grand potentials were calculated as a function of the oxygen chemical potential. Standard DFT, which is known to provide a poor description of the electronic structure of plutonium oxides, predicts an unexpected stabilization of polar uncompensated terminations: O_2-(111), and Pu-(111). We show that this behavior is no longer obtained when the PBE + U framework is used in order to improve the description of the strong electronic correlations that arise in such compounds. Within this approach, we predict one unique stabilized termination over the entire temperature range, regardless of oxygen partial pressure: the O-(111) stoichiometric surface. Consequently, we show that the equilibrium crystal shape of PuO_2 nanocrystals exhibits (111) facets only. This study points out that, a well-suited framework that allows a proper description of strong electronic correlations, such as the PBE + U scheme, is mandatory when *ab initio* calculations of the surface properties of plutonium dioxide are performed. In the future, it would be interesting to extend this work to other strongly correlated, or even slightly correlated, surfaces in order to evaluate the relevancy of such corrections when a modification of the surface electronic structure appears due to vacancy formations, surface chemical reactions, and so on.

ACKNOWLEDGMENTS

We thank Marc Torrent and Bernard Amadon for technical support. All calculations were performed on the TERA-10 supercomputer at Bruyères-le-Châtel (France).

*gerald.jomard@cea.fr

[1] N. Cooper, ed., *Los Alamos Science*, Vol. **26** (Los Alamos National Laboratory, Los Alamos, 2000).
[2] J. L. Sarrao, L. A. Morales, J. D. Thompson, B. L. Scott, G. R. Stewart, F. Wastin, J. Rebizant, P. Boulet, E. Colineau, and G. H. Lander, Nature **420**, 297 (2002).
[3] R. Atta-Fynn and A. K. Ray, Phys. Rev. B **75**, 195112 (2007).
[4] M. Huda and A. Ray, Physica B **352**, 5 (2004).
[5] M. Butterfield *et al.*, Surf. Sci. **600**, 1637 (2006).
[6] J. Bloch and M. Mintz, J. Alloys Compd. **253-254**, 529 (1997).
[7] M. Butterfield, T. Durakiewicz, E. Guziewicz, J. Joyce, A. Arko, K. Graham, D. Moore, and L. Morales, Surf. Sci. **571**, 74 (2004).
[8] C. Colmenares and K. Terada, J. Nucl. Mater. **58**, 336 (1975).
[9] X. Wu and A. K. Ray, Phys. Rev. B **65**, 085403 (2002).
[10] M. Paffett, D. Kelly, S. Joyce, J. Morris, and K. Veirs, J. Nucl. Mater. **322**, 45 (2003).

[11] J. Farr, R. Schulze, and M. Neu, J. Nucl. Mater. **328**, 124 (2004).
[12] M. Brooks, B. Johansson, and H. Skriver, *Handbook on the Physics and Chemistry of the Actinides*, edited by A. J. Freeman and G. H. Lander (North-Holland, New York, 1984), Vol. 1, pp. 153–269.
[13] G. Lander, Science **301**, 1057 (2003).
[14] H. L. Skriver, O. K. Andersen, and B. Johansson, Phys. Rev. Lett. **41**, 42 (1978).
[15] L. Petit, A. Svane, Z. Szotek, and W. Temmerman, Science **301**, 498 (2003).
[16] A. Svane, L. Petit, Z. Szotek, and W. M. Temmerman, Phys. Rev. B **76**, 115116 (2007).
[17] I. Prodan, G. Scuseria, J. Sordo, K. Kudin, and R. Martin, J. Chem. Phys. **123**, 014703 (2005).
[18] I. D. Prodan, G. E. Scuseria, and R. L. Martin, Phys. Rev. B **76**, 033101 (2007).
[19] S. Y. Savrasov and G. Kotliar, Phys. Rev. Lett. **84**, 3670 (2000).
[20] J. Bouchet, B. Siberchicot, F. Jollet, and A. Pasturel, J. Phys. Condens. Matter **12**, 1723 (2000).
[21] A. O. Shorikov, A. V. Lukoyanov, M. A. Korotin, and V. I. Anisimov, Phys. Rev. B **72**, 024458 (2005).
[22] A. Shick, V. Drchal, and L. Havela, Europhys. Lett. **69**, 588 (2005).
[23] A. Shick, L. Havela, J. Kolorenc, V. Drchal, T. Gouder, and P. M. Oppeneer, Phys. Rev. B **73**, 104415 (2006).
[24] B. Sun, P. Zhang, and X.-G. Zhao, J. Chem. Phys. **128**, 084705 (2008).
[25] G. Jomard, B. Amadon, F. Bottin, and M. Torrent, Phys. Rev. B **78**, 075125 (2008).
[26] V. I. Anisimov, J. Zaanen, and O. K. Andersen, Phys. Rev. B **44**, 943 (1991).
[27] V. I. Anisimov, A. I. Poteryaev, M. A. Korotin, A. O. Anokhin, and G. Kotliar, J. Phys. Condens. Matter **9**, 7359 (1997).
[28] A. I. Liechtenstein, V. I. Anisimov, and J. Zaanen, Phys. Rev. B **52**, R5467 (1995).
[29] M. T. Czyżyk and G. A. Sawatzky, Phys. Rev. B **49**, 14211 (1994).
[30] A. Georges, G. Kotliar, W. Krauth, and M. J. Rozenberg, Rev. Mod. Phys. **68**, 13 (1996).
[31] A. I. Lichtenstein and M. I. Katsnelson, Phys. Rev. B **57**, 6884 (1998).
[32] S. Savrasov, G. Kotliar, and E. Abrahams, Nature **410**, 793 (2001).
[33] L. V. Pourovskii, G. Kotliar, M. I. Katsnelson, and A. I. Lichtenstein, Phys. Rev. B **75**, 235107 (2007).
[34] J.-X. Zhu, A. K. McMahan, M. D. Jones, T. Durakiewicz, J. J. Joyce, J. M. Wills, and R. C. Albers, Phys. Rev. B **76**, 245118 (2007).
[35] X. Dai, S. Y. Savrasov, G. Kotliar, A. Migliori, H. Ledbetter, and E. Abrahams, Science **300**, 953 (2003).
[36] C. Noguera, J. Phys. Condens. Matter **12**, R367 (2000).
[37] J. Goniakowski, F. Finocchi, and C. Noguera, Rep. Prog. Phys. **71**, 016501 (2008).
[38] O. Dulub, U. Diebold, and G. Kresse, Phys. Rev. Lett. **90**, 016102 (2003).
[39] The present results have been obtained through the use of the ABINIT code, a common project of the Université Catholique de Louvain, Corning Incorporated, and other contributors, see the URL [http://www.abinit.org].
[40] X. Gonze *et al.*, Comput. Phys. Commun. **180**, 2582 (2009).
[41] M. Torrent, F. Jollet, F. Bottin, G. Zerah, and X. Gonze, Comput. Mater. Sci. **42**, 337 (2008).
[42] N. A. W. Holzwarth, M. Torrent, and F. Jollet, programs ATOMPAW [http://pwpaw.wfu.edu/] and ATOMPAW2ABINIT [http://www.abinit.org] (2007).
[43] H. J. Monkhorst and J. D. Pack, Phys. Rev. B **13**, 5188 (1976).
[44] F. Bottin, S. Leroux, A. Knyazev, and G. Zérah, Comput. Mater. Sci. **42**, 329 (2008).
[45] J. P. Perdew, K. Burke, and M. Ernzerhof, Phys. Rev. Lett. **77**, 3865 (1996).
[46] B. Amadon, F. Jollet, and M. Torrent, Phys. Rev. B **77**, 155104 (2008).
[47] B. Dorado, G. Jomard, M. Freyss, and M. Bertolus, Phys. Rev. B **82**, 035114 (2010).
[48] H. Nakamura, M. Machida, and M. Kato, Phys. Rev. B **82**, 155131 (2010).
[49] K. Reuter and M. Scheffler, Phys. Rev. B **65**, 035406 (2001).
[50] F. Bottin, F. Finocchi, and C. Noguera, Phys. Rev. B **68**, 035418 (2003).
[51] K. Reuter and M. Scheffler, Phys. Rev. B **68**, 045407 (2003).
[52] C.-W. Lee, R. K. Behera, E. D. Wachsman, S. R. Phillpot, and S. B. Sinnott, Phys. Rev. B **83**, 115418 (2011).
[53] K.-P. Bohnen, R. Heid, and O. de la Pena Seaman, Phys. Rev. B **81**, 081405(R) (2010).
[54] M. Valtiner, M. Todorova, G. Grundmeier, and J. Neugebauer, Phys. Rev. Lett. **103**, 065502 (2009).
[55] D. R. Lide, ed., *CRC Handbook of Chemistry and Physics*, 79th ed. (CRC Press, Boca Raton, FL, 1998).
[56] A. Tan, R. Grimes, and S. Owens, J. Nucl. Mater. **344**, 13 (2005).
[57] Y. Jiang, J. Adams, and M. van Schilgaarde, J. Chem. Phys. **123**, 064701 (2005).
[58] X. Wu and A. Ray, Physica B **301**, 359 (2001).
[59] X. Wu and A. Ray, Physica B **293**, 362 (2001).
[60] X. Wu and A. Ray, Eur. Phys. J. B **19**, 345 (2001).
[61] M. Wulff and G. Lander, J. Chem. Phys. **89**, 3295 (1988).
[62] C. McNeilly, J. Nucl. Mater. **11**, 53 (1964).